INNSPUB

International Journal of Biosciences | IJB |
ISSN: 2220-6655 (Print); 2222-5234 (Online)
Website: https://www.innspub.net
Email contact: info@innspub.net
Vol. 27, Issue: 6, p. 14-24, 2025

RESEARCH PAPER OPEN ACCESS

Alpha-tomatine induces ROS-mediated mitochondrial apoptosis in laryngeal carcinoma (HEp-2) cells

Nihal Ahamed Abul Kalam Azad, Suresh Kathiresan*, Theerthu Azhamuthu, Senkuttuvan Ilanchit Chenni, Pugazhendhi Ravichandran, Maharani Jaganathan, Rajeswari Vasu, Pratheeba Veerapandiyan

Department of Biochemistry and Biotechnology, Faculty of Science, Annamalai University, Annamalai Nagar, Tamil Nadu, India

Key words: Alpha-tomatine, Laryngeal carcinoma, Cytotoxicity, ROS, Apoptosis

DOI: https://dx.doi.org/10.12692/ijb/27.6.14-24 Published: December 05, 2025

ABSTRACT

Laryngeal squamous cell carcinoma (LSCC) remains a significant global health challenge, showing minimal improvement in survival rates even with advancements in standard treatments. The growing interest in phytochemicals as potential anticancer agents has highlighted Alpha-tomatine (AT) a steroidal glycoalkaloid derived from tomato plants, because of its strong cytotoxic properties. However, the effects of AT on laryngeal cancer have not been explored previously. This study aims to evaluate the anticancer efficacy of AT in HEp-2 human laryngeal carcinoma cells and to clarify the molecular pathways involved. AT significantly inhibited cell growth in a dose-dependent manner, with an IC_{50} of 29.6 μM. The DCFH-DA staining results showed a marked increase in intracellular reactive oxygen species (ROS), underscoring oxidative stress as a crucial factor in cytotoxicity. Cells treated with AT exhibited significant mitochondrial membrane depolarization (loss of $\Delta\psi m$) and displayed notable apoptotic morphological changes, as evidenced by AO/EtBr and DAPI staining. Results from Annexin V/PI flow cytometry indicated a concentration-dependent increase in both early and late apoptotic cell populations. The comet assay revealed substantial DNA fragmentation, highlighting the genotoxic effects mediated by reactive oxygen species. The findings indicate that AT induces intrinsic apoptosis in HEp-2 cells through mechanisms related to oxidative stress, mitochondrial dysfunction, and DNA damage. These results suggest that AT may be a valuable phytochemical candidate for further investigation as a treatment for laryngeal cancer.

***Corresponding author**: Suresh Kathiresan ✉ suraj_cks@yahoo.co.in

INTRODUCTION

Laryngeal carcinoma represents a common neoplasm of the upper respiratory tract, contributing notably to the overall incidence of head and neck malignancies worldwide. The majority of instances arise from the squamous epithelium located in the glottic, supraglottic, or subglottic regions, with laryngeal squamous cell carcinoma representing 85-90% of total occurrences. The larynx plays a crucial role in voice production, swallowing, and safeguarding the airway, making this malignancy significant in terms of both functionality and clinical outcomes (Fu and Lv, 2024; Hut *et al.*, 2025). Recent global estimates indicate that laryngeal carcinoma impacts around 200,000 individuals each year across the globe, resulting in more than 110,000 fatalities annually (GBD 2019 Respiratory Tract Cancers Collaborators, 2021).

Despite the consistent decrease in age-standardized incidence and mortality rates over the last thirty years, the overall count of laryngeal cancer cases is on the rise primarily driven by population growth and an increasingly older global demographic (Shi *et al.*, 2025). The development of this tumour is strongly influenced by several well-established risk factors, with tobacco and alcohol use being the most significant. Smoking shows a strong dose-dependent increase in risk; smokers are 10–15 times more likely to develop throat cancer than non-smokers, and heavy smokers may face nearly a 30-fold higher risk (He⁺ *et al.*, 2025). Socioeconomic barriers, inadequate access to early diagnostic services, and the high proportion of patients presenting with advanced-stage disease collectively contribute to the poorer survival outcomes observed in many low- and middle-income countries (Zhou *et al.*, 2025). This cancer's survival rates have only slightly improved in recent decades despite advancements in imaging, surgery, radiation, and chemotherapy. Current treatments often cause speech, swallowing, and quality of life issues. Due to late diagnosis, treatment resistance, and high recurrence rates, managing diseases remains difficult (Hut *et al.*, 2025; Rinkel *et al.*, 2016).

In recent years, researchers are currently more interested in the application of phytochemicals, or bioactive substances produced from medicinal plants, as potential alternatives or additional drugs in cancer therapy (Lekhak and Bhattarai, 2024). Phytochemicals possess diverse biological activities, including antioxidant, anti-inflammatory, and potent anticancer properties mediated through modulation of key signaling pathways, induction of apoptosis, inhibition of proliferation, and suppression of metastasis (Rinkel *et al.*, 2016). Their natural source, lower toxicity, and ability to act on multiple biochemical pathways make them promising therapies for existing issues.

Alpha-tomatine (AT) is a natural steroidal glycoalkaloid found in the calyx, leaves, flowers, and especially the unripe fruits of tomato plants, as well as in the roots and tubers of several Solanum species (Fujimaki *et al.*, 2022). Traditionally, AT-rich plants have been valued for their medicinal properties, with many studies reporting strong antitumor and anticancer effects (Echeverría *et al.*, 2022). Beyond its anticancer potential, AT exhibits multiple pharmacological activities, including anti-inflammatory (Zhao *et al.*, 2015), antibacterial (Tam *et al.*, 2021), antimalarial (Chen *et al.*, 2010), antioxidant (Silva-Beltrán *et al.*, 2015), anticarcinogenic and cardioprotective effects (Friedman, 2013). These various activities highlight AT's importance as a multifunctional bioactive molecule with promising therapeutic applications.

Early investigations revealed that AT exhibits strong cytotoxicity against a variety of human cancer cell lines, including prostate (PC-3) (Lee *et al.*, 2011), lung (A549) (Shih *et al.*, 2009), leukemia HL-60 (Huang *et al.*, 2015), breast MCF-7 (Sucha *et al.*, 2013), hepatocellular carcinoma (HepG2) and colon (HT-29) (Lee *et al.*, 2004). AT significantly inhibited the growth and development of human gastric cancer cells, which display various differentiation states and resistance to cisplatin, by effectively targeting the PI3K-AKT and MAPK signaling pathways (Zhang *et al.*, 2020). AT significantly reduced the activation of signaling

pathways associated with non-small-cell lung cancer and modulated the elevated expression of the EGFR protein (Brawijaya University, 65145 *et al.*, 2020).

Although AT exhibits several anti-tumor activities in numerous cancer cell types, its anticancer potential and the associated molecular and biological processes in laryngeal carcinoma remain uninvestigated. The current study is the first to examine the effects of AT on HEp-2 cancer cells, highlighting vital pathways such as ROS generation, impairment of mitochondrial membrane potential (MMP), nuclear damage, DNA fragmentation, and apoptotic changes that lead to cell death.

MATERIALS AND METHODS

Chemicals

Dulbecco's Modified Eagle Medium (DMEM), Fetal bovine serum (FBS), 0.25% trypsin-EDTA, antibiotics (streptomycin, penicillin), phosphate-buffered saline (PBS), ethanol, methanol, dimethyl sulfoxide (DMSO), sodium dodecyl sulfate (SDS). N, N, N′, N′-tetramethylene diamine (TEMED), bovine serum albumin (BSA), and 2-mercaptoethanol were purchased from Hi-media Lab. Alpha-tomatine (≥95% (HPLC), 3-(4,5-dimethylthiazol-2-yl) −2,5-diphenyl tetrazolium bromide (MTT), 2,7-diacetyl dichlorofluorescein diacetate (DCFH-DA), Rhodamine 123, 6-diamidino-2-phenylindole (DAPI), Ethidium Bromide (EtBr), and Acridine Orange (A/O) were all acquired from Sigma-Aldrich. Primary antibodies such as p53, Caspase-3, Caspase-9, Bcl2, Bax and β-actin and secondary antibodies were acquired from Santa Cruz Biotechnology (SCBT) and Cell Signaling Technology (CST).

Cell growth and maintenance

The human laryngeal carcinoma cell line (Hep-2) were purchased from the National Centre for Cell Science (NCCS), Pune, and cultured in a single layer in a T25 cm^2 flask using DMEM Medium containing FBS (10%), glutamine (1%), 100 Ug/mL streptomycin-penicillin at 37°C and 5% CO_2 in an incubator.

Preparation of alpha-tomatine

Alpha-tomatine (AT) was dissolved in 10% dimethyl sulfoxide (DMSO) and diluted in complete culture medium to achieve final concentrations of 1to100 µM. Cells were treated with AT and incubated for 24 h.

Cell cytotoxicity assay

The human laryngeal carcinoma cell line HEp-2 were cultured at concentration 1× 10^4 cells/well on white flat-bottom 96-well plates and treatment with AT at concentrations ranging from 1 to 100 µM. After 24-h incubation at 37°C, 10 µL of MTT solution (5 mg/mL) were added to each well to facilitate low-light absorption. After a 4h incubation, the MTT reagent was carefully eliminated, and an addition of 100 µL of DMSO to each well resulted in the formation of a purple formazan crystal structure. The absorbance required for cell viability has been measured at 570 nm with a multimode reader (Molecular Devices, USA) (Azhamuthu *et al.*, 2024a). Percentage of viability was determined as follows.

$$\% \text{ Viability} = \frac{Total\ number\ of\ viable\ cells}{Total\ number\ of\ viable\ and\ nonviable\ cells} \times 100$$

Evaluation of intracellular ROS production

The DCFH-DA staining method were used to measure the amount of ROS (reactive oxygen species) in HEp-2 cells after they were treated with AT at various concentrations of 10, 20, and 30 µM, and cells were maintained for 24 h. Cells in both the control and experimental groups were stained with DCFH-DA (10 µM) and kept at 37°C for 30 minutes in the dark place. Intracellular ROS levels were measured at 485±10 and 530±12.5 nm using a multimode reader and the images were obtained using a fluorescence microscope (Floid system for cell imaging; Life Technologies) (Venkatachalam *et al.*, 2024).

Assessment of mitochondrial membrane potential (Δψm)

Mitochondrial membrane potential was evaluated using Rhodamine 123 (Rh-123). Fluorescent dye that easily penetrates cell membranes and has a negative

charge, enabling its absorption by the mitochondrial membrane. Rh-123 cannot penetrate the mitochondrial membrane when its potential is diminished. HEp-2 cells were grown in a 12-well plate and exposed to varying concentration of AT 10, 20 and 30 µM for 24 h. Rh-123 was used at a final concentration of 10 µM and incubated for 30 minutes at 37°C in darkness. The cells were subsequently rinsed with PBS and examined using a fluorescence microscope (Chao *et al.*, 2012).

DAPI staining with nuclear morphology assessment

DAPI nuclear labelling was employed to assess the nuclear morphological alterations induced by AT in HEp-2 cells. Cells were grown in 6-well plates, treated with 10, 20 and 30 µM AT at 37°C with 5% CO_2 for 24 h. Following incubation, the cells were stained with DAPI at a concentration of 1 mg/mL and kept in the dark place for 30 minutes. After the period of incubation, the labelled malignant cells expose through analysis under a fluorescence microscope (Qian *et al.*, 2021).

Assessment of apoptotic morphological alterations

HEp-2 cells were treated with different concentrations of 10, 20 and 30 µM of AT for 24 h. After incubation, the DMEM medium was removed and rinsed twice with PBS. The cells were preserved with formaldehyde over 30 min at 4°C. Subsequently, the cells were rinsed with PBS then treated in 1:1 solution of AO/EtBr for 30 min at 37°C in the dark place. The number of cells exhibiting apoptotic features were determined after the stained cells washed with PBS (Gheena and Ezhilarasan, 2019).

Annexin-V/propidium iodide (PI) staining

Annexin-V/PI staining was performed to assess early and late apoptosis in HEp-2 cells treated with AT (10, 20, and 30 µM) for 24 h. After incubation, cells were harvested, washed with PBS, and stained with Annexin-V (1 µg/mL) and PI (1 µg/mL) in binding buffer for 15 min at room temperature. Flow cytometric analysis was carried out using a CytoFLEX S (Beckman Coulter, USA), recording 1 × 10^4 events per sample, including both live and dead cells.

Analysing DNA damage using comet assay

Comet assay was utilized for DNA fragmentation assessment in HEp-2 cells due to its efficiency and reliability in detecting damage to the DNA structure. Briefly, HEp-2 cells were grown in 6-well plates and treated with AT at doses of 10, 20 and 30 µM for 24 h. Following treatment, the cells were collected, rinsed with chilled PBS, centrifuged, and subsequently suspended in PBS while kept on ice. Low-melting agarose (1% w/v) was dissolved in a boiling water bath at 90–95°C for 20 min and subsequently cooled to 37°C. Cells were mixed with low-melting agarose at a ratio of 1:10, After comet slides were prepared with 50 µl aliquots of the mixture. The slides were then put into lysis buffer (10× lysis, NaCl, EDTA, H_2O, pH 10) for 30 mins (dark place at 40°C), creating a lysis buffer incubation during the cold alkaline solution treatment. And then put slanted in an electrophoresis chamber and run at 1 V for 10-15 mins. Slides were fixed in 70% ethanol and washed multiple times with water. Cells were examined and photographed using a fluorescence microscope after staining the cellular DNA with ethidium bromide (Syed *et al.*, 2018).

Statistical analysis

The results were obtained in triplicate and presented as mean ± SD (n=3). The IC_{50} (half of the maximal inhibitory concentration) was determined using GraphPad Prism (GraphPad application, Version 10.0.0, San Diego, USA). A one- and two-way ANOVA test ($\alpha = 0.05$) was used to compare group means, demonstrating the statistical significance determined by Tukey's test.

RESULTS

AT inhibits cell proliferation in HEp-2 cells

The MTT assay was utilized to evaluate the efficacy of AT as a cytotoxic agent on HEp-2 cells. Fig. 1

demonstrates that AT was evaluated on HEp-2 cells at concentrations varying from 1 to 100 µM. The incubation period was extended by 24 hours, illustrating both dose-dependent and time-dependent cytotoxic effects of AT on HEp-2 cells. The cell inhibition rate attained 50% (IC50) at a concentration of 29.6 µM following a 24-hour incubation under the designated conditions. The findings resulted in the selection of AT concentrations of 10, 20, and 30 µM for subsequent study and analysis.

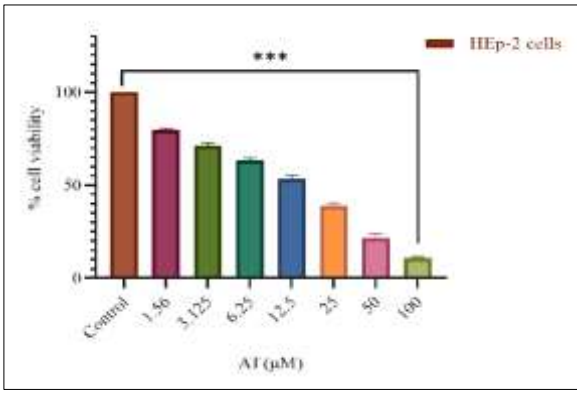

Fig. 1. The effect of AT on HEp-2 cell viability was evaluated using the MTT assay after 24 h of treatment with concentrations ranging from 1 to 100 µM. The results are presented as mean ± SD (n = 3), with ***p < 0.001 indicating a statistically significant reduction in viability compared with the control group.

AT induced ROS generation in HEp-2 cells

Early results indicate that AT could possess anticancer effects by increasing oxidative damage. The fluorescence intensity of DCFH-DA within HEp-2 cells reflected the effect of AT on intracellular ROS generation following 24 hours of treatment. The findings revealed that AT, at concentrations of 10, 20, and 30 µM, considerably increased ROS generation in HEp-2 cells in a dose-dependent manner compared to the control group. The statistical analyses found that varying concentrations of AT 10, 20, and 30 µM enhanced ROS production in these tumor cells, with corresponding increases in fluorescence intensity compared to the untreated cells. The elevated production of reactive oxygen species after AT treatment indicates that oxidative stress may have triggered apoptosis (Fig. 2A & 2B).

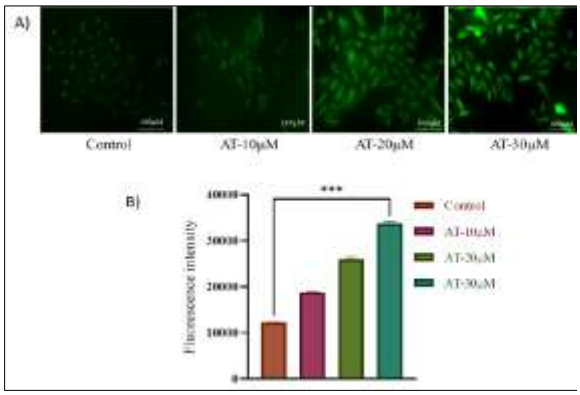

Fig. 2. Effect of AT persuades intracellular ROS in Hep-2 cells using the staining method (DCFH-DA). a) The AT-treated Hep-2 cells exhibit increased green fluorescence in a photomicrograph using a green light source. b) Bar diagram shows the percentage of fluorescence intensity under excitation and emission wavelength at 485 ± 10 and 530 ± 12.5 nm, respectively. Data represent mean values ± SD, where n = 3 and ***p < 0.001 when compared with control. Scale bar = 100 µM.

AT induced Δψm in HEp-2 cells

A study examining changes in mitochondrial membrane potential (Δψm) in HEp-2 cells has been performed using Rh-123 staining (Fig. 3).

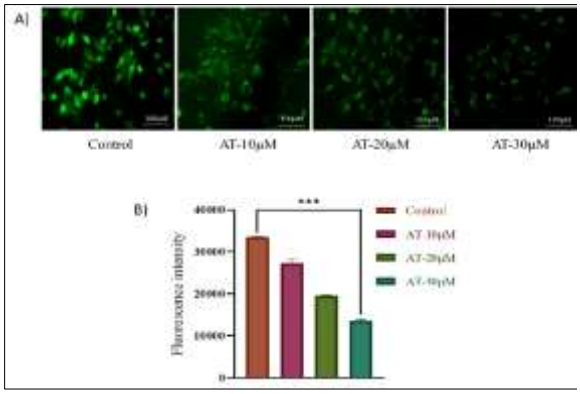

Fig. 3. Effect of AT on MMP level by Rh-123 stain method. (a) The photomicrograph of AT-treated Hep-2 cells depicts a decrease in green fluorescence intensity with loss of mitochondrial membrane potential. (b) The bar graph shows the percentage of fluorescence intensity measured using a multimode reader. Data represent mean values ± SD, where n = 3 and ***p < 0.001 when compared with control. Scale bar = 100 µM.

The evaluation of apoptotic cell death in carcinoma cells depends on modifications to Δψm. Fluorescence microscopy studies reveal that, in the presence of a polarized mitochondrial membrane, untreated cells show no early signs of death. The reduced green fluorescence suggested that cells subjected to varying AT concentrations of 10, 20, and 30 µM displayed the most noticeable signs of cell death. As a result, when there is a change in Δψm, the fluorescence intensity of the Rh-123 label diminishes as the concentration increases. The administration of various doses of AT to HEp-2 cells led to a significant decrease in green fluorescence at all levels, along with a marked change in Δψm (Fig. 3A & 3B).

AT induces apoptosis as evidenced by morphological changes in HEp-2 cells

Rh-123 labeling has been utilized to investigate changes in mitochondrial membrane potential (Δψm) in HEp-2 cells. Alterations in Δψm are essential for evaluating apoptotic cell death in cancer cells. Research using fluorescence microscopy indicates that untreated cells do not show early signs of death while the mitochondrial membrane remains polarized. In contrast, cells exposed to varying concentrations of AT specifically 10, 20, and 30 µM demonstrated clear signs of cell death, as evidenced by the reduced green fluorescence. Therefore, as the concentration increases, the fluorescence intensity of the Rh-123 label decreases alongside changes in Δψm. At all concentrations tested, green fluorescence significantly diminished when different dosages of AT were applied to HEp-2 cells, resulting in notable alterations to Δψm (Fig. 4A&B).

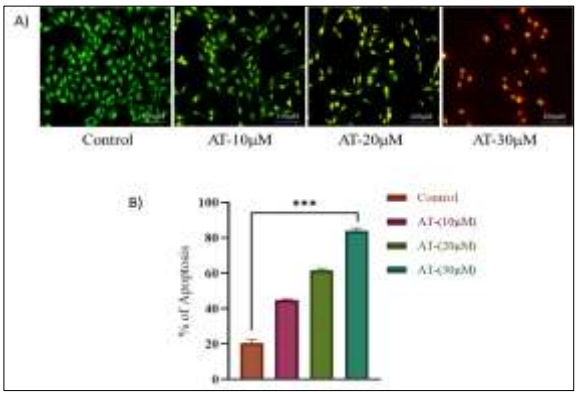

Fig. 4. Effect of AT on apoptotic changes using AO/EtBr. (a) Dual staining found apoptotic morphological characteristic alterations in AT-treated cells. (b) The percentage of apoptotic cells in AT-treated Hep-2 cells were measured. Data represent mean values ± SD, where n = 3 and $^{***}p < 0.001$ when compared with control. Scale bar = 100 µM.

AT induces apoptosis in Hep-2 Cells as determined by Annexin V/PI flow cytometry

Annexin V-FITC/PI dual staining followed by flow cytometry was used to quantify apoptosis in HEp-2 cells treated with increasing concentrations of AT (10, 20, and 30 µM) compared with the untreated control. In the control group, most cells remained viable (67.28%, Q1-LL), with only a small fraction undergoing apoptosis (7.70%, Q1-UR) (Fig. 5A).

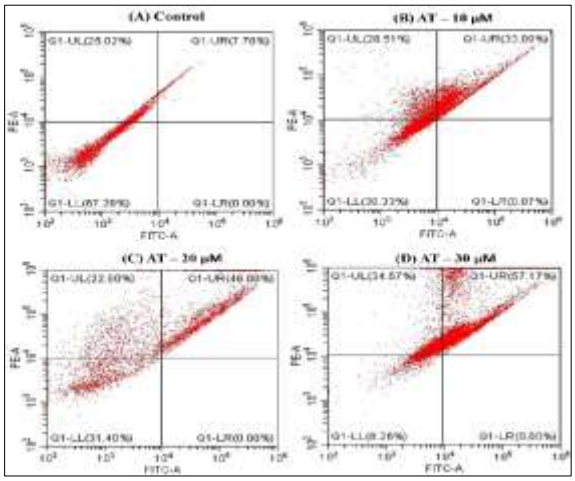

Fig. 5. Effect of AT on apoptotic induction in Hep-2 cells using Annexin V/PI staining. Flow cytometry analysis showing apoptotic cell populations in (A) control and AT-treated cells at concentrations of (B) 10 µM, (C) 20 µM, and (D) 30 µM for 24 h. Quadrant distribution: Q1-LL (Annexin V^-/PI^-, viable cells), Q1-LR (Annexin V^+/PI^-, early apoptotic cells), Q1-UR (Annexin V^+/PI^+, late apoptotic/necrotic cells), and Q1-UL (Annexin V^-/PI^+, necrotic cells).

AT treatment resulted in a clear dose-dependent increase in apoptotic cell populations. At 10 µM, both early and late apoptosis increased markedly, with late apoptotic cells reaching 33.09% (Q1-UR) (Fig. 5B). Increasing the concentration to 20 µM further elevated apoptosis, with 46% of cells in the late apoptotic quadrant (Fig. 5C). At 30 µM, the

majority of cells (57.17%) shifted to late apoptosis, indicating substantial apoptotic induction (Fig. 5D). Overall, these results demonstrate that AT potently triggers apoptosis in HEp-2 cells in a concentration-dependent manner.

Effect of AT induces nuclear condensation in HEp-2 cell line

We evaluated the effect of AT treatment on nuclear condensation in HEp-2 cells following exposure to 10, 20, and 30 µM for 24 h. Untreated control cells showed no signs of nuclear condensation, as indicated by the low-intensity DAPI fluorescence typical of healthy nuclei. In contrast, cells treated with lower concentrations of AT exhibited mild increases in DAPI fluorescence, reflecting early apoptosis. Higher concentrations of AT induced a pronounced rise in DAPI intensity, corresponding to late-stage apoptotic changes. Overall, AT treatment resulted in markedly enhanced nuclear condensation and fragmentation in HEp-2 cells compared to the controls (Fig. 6).

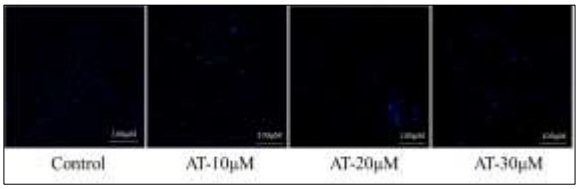

Fig. 6. Shows apoptotic morphological changes DAPI staining were observed in control and AT treated cells. The different concentration (10, 20 and 30 µM) of AT treated Hep-2 cells shows increased fragmented nuclei and membrane blebbing. Scale bar = 100 µM.

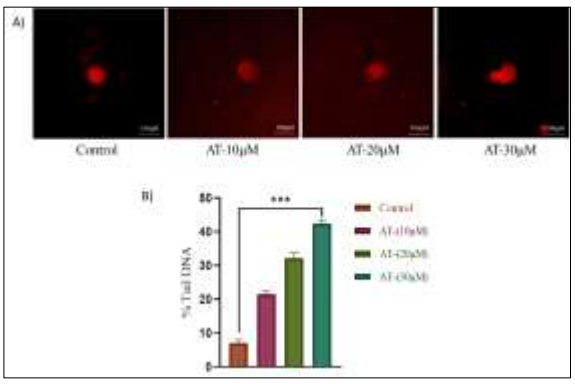

Fig. 7. (a) The standard fluorescent microscopic image of AT-treated Hep-2 comet cells following alkaline gel electrophoresis is displayed due to DNA damage. (b) The percentage of tail DNA shows DNA damage in AT-treated Hep-2 cells, were calculated by CASP software. Data represent mean values ± SD, where n = 3 and ***p < 0.001 when compared with control. Scale bar = 100 µM.

Assessment of DNA damage by comet assay

Comet assay analysis revealed a progressive increase in DNA fragmentation in HEp-2 cells following AT treatment at 10, 20, and 30 µM (Fig. 7A & 7B). This was evidenced by a concentration-dependent reduction in comet head DNA and a corresponding increase in comet tail DNA. The highest level of DNA damage was observed at 30 µM. In contrast, the control group exhibited intact DNA, characterized by well-defined comet heads with negligible or absent tails.

DISCUSSION

The current investigation demonstrates that α-tomatine possesses significant anticancer properties against HEp-2 cells via various associated mechanisms, including inhibition of cell proliferation, enhancement of oxidative stress, impairment of mitochondrial function, initiation of apoptosis, and induction of DNA damage. The MTT assay results demonstrated that AT significantly inhibited the proliferation of HEp-2 cells in a clear dose-dependent manner, with an IC_{50} value of 29.6 µM after 24 hours. Prior studies have demonstrated that AT possesses significant cytotoxic properties against diverse cancer cell lines, with IC50 values around 1.67 µM in PC-3 prostate cancer cells. Breast cancer MCF-7 cells demonstrate IC50 value 7.17 µM (Lee *et al.*, 2011; Sucha *et al.*, 2013). The initial reduction in cell viability guided the selection of optimal working concentrations of 10, 20, and 30 µM for subsequent experiments.

The main factor contributing to AT-induced cytotoxicity is oxidative stress, evidenced by the significant increase in intracellular ROS generation following DCFH-DA staining. Increased amounts of ROS are known to induce intrinsic apoptosis, which typically results in mitochondrial depolarization and increased DNA fragmentation (De Haan *et al.*, 2022; Kim and Xue, 2020).

The results of the ROS assay support this oxidative mechanism.

Rhodamine 123 staining was employed to evaluate the effect of α-tomatine (AT) on mitochondrial membrane potential (Δψm) in HEp-2 cells. Rh-123 is a cationic and lipophilic fluorescent dye that primarily accumulates in mitochondria with intact and highly polarized membranes, resulting in high fluorescence under normal conditions. HEp-2 cells treated with AT, there was a significant reduction in Rh-123 fluorescence, indicating mitochondrial depolarization. The loss of Δψm represents an early and crucial event in the intrinsic apoptotic pathway, signaling a breakdown in mitochondrial integrity (Lu *et al.*, 2018; Zorova *et al.*, 2022). The AT-induced depolarization of mitochondria demonstrates its capacity to disrupt mitochondrial function, highlighting the role of mitochondrial-mediated apoptosis in the cytotoxic response observed in HEp-2 cells.

The application of AO/EtBr staining for morphological evaluations yielded distinct visual indicators of apoptosis. The AT treated cells displayed characteristics indicative of both early and late stages of apoptosis, such as membrane blebbing, chromatin condensation, and distinct orange/red fluorescence patterns. The observed morphological transitions became more pronounced as AT concentration raised, indicating the advancement of apoptotic processes (Annamalai *et al.*, 2016). Similar results were observed with DAPI staining, where AT-treated cells exhibited significant nuclear condensation and fragmentation key indicators of late-stage apoptosis. The enhanced nuclear fluorescence observed at elevated concentrations confirmed considerable chromatin disruption, supporting the findings related to the induction of apoptosis (Azhamuthu *et al.*, 2024b).

Annexin V-FITC, a phosphatidylserine-binding probe, can be conjugated to fluorescent tags and used alongside propidium iodide (PI), a dye that penetrates only non-viable cells, for flow cytometric detection of apoptotic and dead cells (Pumiputavon *et al.*, 2017). In this study, flow cytometry of untreated HEp-2 cells revealed minimal Annexin V-FITC and PI staining, confirming that most cells remained viable. In contrast, exposure to increasing concentrations of AT for 24 hours resulted in a marked shift in cell populations. A dose-dependent rise in Annexin V- and/or PI-positive cells was observed, demonstrating that AT efficiently triggers apoptosis in HEp-2 cells.

The Comet assay provided additional confirmation of the genotoxic effects resulting from AT treatment. HEp-2 cells exhibited a progressive enhancement in comet tail length alongside a decrease in comet head DNA, signifying significant DNA strand breaks. This pattern reflects the oxidative DNA damage induced by reactive oxygen species, which is frequently linked to intrinsic apoptotic pathways. The most significant DNA fragmentation was observed at the highest concentration 30 µM, which aligned with increased levels of reactive oxygen species and mitochondrial impairment (Kúdelová *et al.*, 2013). The comprehensive experimental results indicate that α-tomatine holds significant promise as a therapeutic candidate for laryngeal cancer. This finding indicates that it requires additional in vivo validation and a deeper investigation into its mechanisms to enhance its potential for clinical application.

CONCLUSION

This investigation reveals that AT displays potent anticancer properties against HEp-2 laryngeal carcinoma cells via various interconnected mechanisms. AT reported a dose-dependent inhibition of cell proliferation and markedly increased intracellular ROS levels, resulting in oxidative stress. This change was associated with mitochondrial depolarization, morphological changes indicative of apoptosis, and a rise in Annexin V/PI-positive cells, thereby confirming the activation of intrinsic apoptosis. The comet assay demonstrated significant DNA fragmentation, highlighting the genotoxic effects linked to the increase in ROS levels. The findings collectively represent AT as a promising candidate for additional investigation as a therapeutic agent in the context of laryngeal cancer.

ACKNOWLEDGEMENTS

The authors gratefully acknowledge the Rashtriya Uchchatar Shiksha Abhiyan (RUSA), Government of India, for financial supporting to Dr. K. Suresh under Rashtriya Uchchatar Shiksha Abhiyan (RUSA) Scheme [File Ref. No. 306]. This work was done by Mr. A. Nihal Ahamed is the project fellow in this project.

REFERENCES

Amalia IF, Sayyidah A, Larasati KA, Budiarti SF. 2020. Molecular docking analysis of α-tomatine and tomatidine to inhibit epidermal growth factor receptor activation in non-small-cell lung cancer (NSCLC). JSMARTech **2**(1), 001–006. https://doi.org/10.21776/ub.jsmartech.2020.002.01.1

Annamalai G, Kathiresan S, Kannappan N. 2016. [6]-Shogaol, a dietary phenolic compound, induces oxidative stress-mediated mitochondrial-dependent apoptosis through activation of proapoptotic factors in Hep-2 cells. Biomedicine & Pharmacotherapy **82**, 226–236. https://doi.org/10.1016/j.biopha.2016.04.044

Azhamuthu T, Kathiresan S, Senkuttuvan I, Asath NAA, Ravichandran P, Vasu R. 2024a. Usnic acid alleviates inflammatory responses and induces apoptotic signaling through inhibiting NF-κB expression in human oral carcinoma cells. Cell Biochemistry and Function **42**(4), e4074. https://doi.org/10.1002/cbf.4074

Azhamuthu T, Kathiresan S, Senkuttuvan I, Asath NAA, Ravichandran P, Vasu R. 2024b. Usnic acid alleviates inflammatory responses and induces apoptotic signaling through inhibiting NF-κB expression in human oral carcinoma cells. Cell Biochemistry and Function **42**(4), e4074. https://doi.org/10.1002/cbf.4074

Chao M-W, Chen C-H, Chang Y-L, Teng C-M, Pan S-L. 2012. α-Tomatine-mediated anticancer activity *in vitro* and *in vivo* through cell-cycle- and caspase-independent pathways. PLOS ONE **7**, e44093. https://doi.org/10.1371/journal.pone.0044093

Chen Y, Li S, Sun F, Han H, Zhang X, Fan Y, Tai G, Zhou Y. 2010. *In vivo* antimalarial activities of glycoalkaloids isolated from Solanaceae plants. Pharmaceutical Biology **48**(9), 1018–1024. https://doi.org/10.3109/13880200903440211

De Haan LR, Reiniers MJ, Reeskamp LF, Belkouz A, Ao L, Cheng S, Ding B, Van Golen RF, Heger M. 2022. Experimental conditions that influence the utility of 2′,7′-dichlorodihydrofluorescein diacetate ($DCFH_2$-DA) as a fluorogenic biosensor for mitochondrial redox status. Antioxidants **11**(8), 1424. https://doi.org/10.3390/antiox11081424

Echeverría C, Martin A, Simon F, Salas CO, Nazal M, Varela D, Pérez-Castro RA, Santibanez JF, Valdés-Valdés RO, Forero-Doria O, Echeverría J. 2022. *In vivo* and *in vitro* antitumor activity of tomatine in hepatocellular carcinoma. Frontiers in Pharmacology **13**, 1003264. https://doi.org/10.3389/fphar.2022.1003264

Friedman M. 2013. Anticarcinogenic, cardioprotective, and other health benefits of tomato compounds lycopene, α-tomatine, and tomatidine in pure form and in fresh and processed tomatoes. Journal of Agricultural and Food Chemistry **61**(40), 9534–9550. https://doi.org/10.1021/jf402654e

Fu Z, Lv J. 2024. Commentary on "Updated disease distributions, risk factors, and trends of laryngeal cancer: a global analysis of cancer registries." International Journal of Surgery **110**(7), 4435–4436. https://doi.org/10.1097/JS9.0000000000001355

Fujimaki J, Sayama N, Shiotani S, Suzuki T, Nonaka M, Uezono Y, Oyabu M, Kamei Y, Nukaya H, Wakabayashi K, Morita A, Sato T, Miura S. 2022. The steroidal alkaloid tomatidine and tomatidine-rich tomato leaf extract suppress the human gastric cancer-derived 85As2 cells in vitro and in vivo via modulation of interferon-stimulated genes. Nutrients **14**(5), 1023. https://doi.org/10.3390/nu14051023

GBD 2019 Respiratory Tract Cancers Collaborators. 2021. Global, regional, and national burden of respiratory tract cancers and associated risk factors from 1990 to 2019: a systematic analysis for the Global Burden of Disease Study 2019. The Lancet Respiratory Medicine **9**(9), 1030–1049. https://doi.org/10.1016/S2213-2600(21)00164-8

Gheena S, Ezhilarasan D. 2019. Syringic acid triggers reactive oxygen species–mediated cytotoxicity in HepG2 cells. Human & Experimental Toxicology **38**(6), 694–702. https://doi.org/10.1177/0960327119839173

He Z, Hu Y, Yang X, Han B, Li S, Huang S, Chen X. 2025. Global trends and cross-country inequalities in laryngeal cancer: a systematic analysis of the 2021 Global Burden of Disease study represented by China. Tobacco Induced Diseases **23**, 1–16. https://doi.org/10.18332/tid/205796

Huang H, Chen S, Van Doren J, Li D, Farichon C, He Y, Zhang Q, Zhang K, Conney AH, Goodin S, Du Z, Zheng X. 2015. α-Tomatine inhibits growth and induces apoptosis in HL-60 human myeloid leukemia cells. Molecular Medicine Reports **11**(6), 4573–4578. https://doi.org/10.3892/mmr.2015.3238

Hut A-R, Boia ER, Para D, Iovanescu G, Horhat D, Mikša L, Chiriac M, Galant R, Motofelea AC, Balica NC. 2025. Laryngeal cancer in the modern era: evolving trends in diagnosis, treatment, and survival outcomes. Journal of Clinical Medicine **14**(10), 3367. https://doi.org/10.3390/jcm14103367

Kim H, Xue X. 2020. Detection of total reactive oxygen species in adherent cells by 2′,7′-dichlorodihydrofluorescein diacetate staining. Journal of Visualized Experiments **160**, 60682. https://doi.org/10.3791/60682

Kúdelová J, Seifrtová M, Suchá L, Tomšík P, Havelek R, Řezáčová M. 2013. α-Tomatine activates cell cycle checkpoints in the absence of DNA damage in human leukemic MOLT-4 cells. Journal of Applied Biomedicine **11**(2), 93–103. https://doi.org/10.2478/v10136-012-0033-8

Lee K-R, Kozukue N, Han J-S, Park J-H, Chang E, Baek E-J, Chang J-S, Friedman M. 2004. Glycoalkaloids and metabolites inhibit the growth of human colon (HT29) and liver (HepG2) cancer cells. Journal of Agricultural and Food Chemistry **52**(10), 2832–2839. https://doi.org/10.1021/jf030526d

Lee S-T, Wong P-F, Cheah S-C, Mustafa MR. 2011. α-Tomatine induces apoptosis and inhibits nuclear factor-κB activation in human prostatic adenocarcinoma PC-3 cells. PLOS ONE **6**(4), e18915. https://doi.org/10.1371/journal.pone.0018915

Lekhak N, Bhattarai HK. 2024. Phytochemicals in cancer chemoprevention: preclinical and clinical studies. Cancer Control **31**, 10732748241302902. https://doi.org/10.1177/10732748241302902

Lu J, Wu L, Wang X, Zhu J, Du J, Shen B. 2018. Detection of mitochondrial membrane potential to study CLIC4 knockdown-induced HN4 cell apoptosis *in vitro*. Journal of Visualized Experiments **137**, 56317. https://doi.org/10.3791/56317

Pumiputavon K, Chaowasku T, Saenjum C, Osathanunkul M, Wungsintaweekul B, Chawansuntati K, Wipasa J, Lithanatudom P. 2017. Cell cycle arrest and apoptosis induction by methanolic leaf extracts of four Annonaceae plants. BMC Complementary and Alternative Medicine **17**(1), 294. https://doi.org/10.1186/s12906-017-1811-3

Qian S, Fang H, Zheng L, Liu M. 2021. Zingerone suppresses cell proliferation via inducing cellular apoptosis and inhibition of the PI3K/AKT/mTOR signaling pathway in human prostate cancer PC-3 cells. Journal of Biochemical and Molecular Toxicology **35**(1), e22611. https://doi.org/10.1002/jbt.22611

Rinkel RN, Verdonck-de Leeuw IM, Doornaert P, Buter J, De Bree R, Langendijk JA, Aaronson NK, Leemans CR. 2016. Prevalence of swallowing and speech problems in daily life after chemoradiation for head and neck cancer based on SWAL-QOL and SHI. European Archives of Oto-Rhino-Laryngology **273**(7), 1849–1855. https://doi.org/10.1007/s00405-015-3680-z

Shih Y-W, Shieh J-M, Wu P-F, Lee Y-C, Chen Y-Z, Chiang T-A. 2009. α-Tomatine inactivates PI3K/Akt and ERK signaling pathways in human lung adenocarcinoma A549 cells: effect on metastasis. Food and Chemical Toxicology **47**(8), 1985–1995. https://doi.org/10.1016/j.fct.2009.05.011

Silva-Beltrán NP, Ruiz-Cruz S, Cira-Chávez LA, Estrada-Alvarado MI, Ornelas-Paz JJ, López-Mata MA, Del-Toro-Sánchez CL, Ayala-Zavala JF, Márquez-Ríos E. 2015. Total phenolic, flavonoid, tomatine, and tomatidine contents and antioxidant and antimicrobial activities of tomato plant extracts. International Journal of Analytical Chemistry **2015**, 284071. https://doi.org/10.1155/2015/284071

Sucha L, Hroch M, Řezáčová M, Rudolf E, Havelek R, Šípera L, Cmielová J, Kohlerová R, Bezrouk A, Tomšík P. 2013. Cytotoxic effect of α-tomatine in MCF-7 human breast cancer cells depends on cholesterol interaction and does not involve apoptosis. Oncology Reports **30**(6), 2593–2602. https://doi.org/10.3892/or.2013.2778

Syed FQ, Elkady AI, Mohammed FA, Mirza MB, Hakeem KR, Alkarim S. 2018. Chloroform fraction of Foeniculum vulgare induces ROS-mediated mitochondria-caspase-dependent apoptosis in MCF-7 cells. Journal of Ethnopharmacology **218**, 16–26. https://www.sciencedirect.com/science/article/pii/S0378874117346123

Tam CC, Nguyen K, Nguyen D, Hamada S, Kwon O, Kuang I, Gong S, Escobar S, Liu M, Kim J, Hou T, Tam J, Cheng LW, Kim JH, Land KM, Friedman M. 2021. Antimicrobial properties of tomato leaves, stems, and fruit and their relationship to chemical composition. BMC Complementary Medicine and Therapies **21**(1), 229. https://doi.org/10.1186/s12906-021-03391-2

Venkatachalam J, Jeyadoss VS, Bose KSC, Subramanian R. 2024. Marine seaweed endophytic fungi-derived metabolites promote ROS-induced cell cycle arrest and apoptosis in human breast cancer cells. Molecular Biology Reports **51**(1), 611. https://doi.org/10.1007/s11033-024-09511-8

Zhang D, Yuan H, Mo S-S, Mo X-W, Tang W-Z, Yan L-H. 2020. α-Tomatine inhibits proliferation, metastasis, drug resistance and immune infiltration through the PI3K-AKT-MAPK axis in gastric cancer. Research Square Preprint. https://doi.org/10.21203/rs.3.rs-53224/v1

Zhao B, Zhou B, Bao L, Yang Y, Guo K. 2015. α-Tomatine exhibits anti-inflammatory activity in lipopolysaccharide-activated macrophages. Inflammation **38**(5), 1769–1776. https://doi.org/10.1007/s10753-015-0154-9

Zhou T, Wang X, Zhu Q, Zhou E, Zhang J, Song F, Xu C, Shen Y, Zou J, Zhu H, Su K, Lu W, Yi H, Huang W. 2025. Global trends and risk factors of laryngeal cancer: a systematic analysis for the Global Burden of Disease Study (1990–2021). BMC Cancer **25**(1), 296. https://doi.org/10.1186/s12885-025-13700-4

Zorova LD, Demchenko EA, Korshunova GA, Tashlitsky VN, Zorov SD, Andrianova NV, Popkov VA, Babenko VA, Pevzner IB, Silachev DN, Plotnikov EY, Zorov DB. 2022. Is the mitochondrial membrane potential (ΔΨ) correctly assessed? intracellular and intramitochondrial modifications of the ΔΨ probe rhodamine 123. International Journal of Molecular Sciences **23**(1), 482. https://doi.org/10.3390/ijms23010482